Supplementary: Reforestation scenarios shape global and regional temperature outcomes

Nora L. S. Fahrenbach[1*], Steven J. De Hertog[2], Felix Jäger[1], Peter J. Lawrence[3], Robert C. Jnglin Wills[1]

[1*]Institute for Atmospheric and Climate Science, ETH Zurich, Universitaetstrasse 16, Zurich, 8092, Switzerland.
[2]Q-ForestLab, Department of Environment, Ghent University, Coupure links 653, Ghent, 9000, Belgium.
[3]Climate and Global Dynamics Laboratory, National Center for Atmospheric Research, 1850 Table Mesa Drive Boulder, Boulder, 80305, Colorado, USA.

*Corresponding author(s). E-mail(s): nora.fahrenbach@env.ethz.ch;
Contributing authors: steven.dehertog@ugent.be; felix.jaeger@env.ethz.ch; lawrence@ucar.edu; robert.jnglinwills@env.ethz.ch;

1 Land carbon changes following reforestation potentials

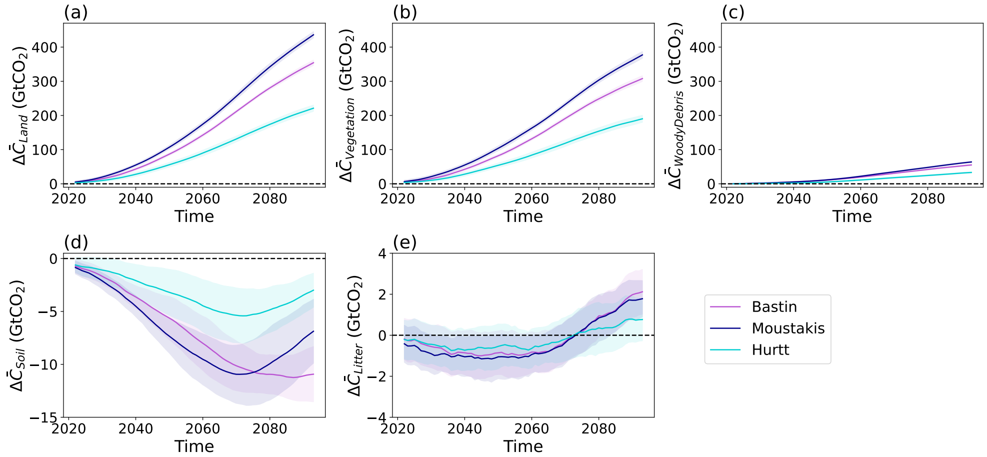

Fig. S1 Time series of global-mean changes in (a) land carbon $\bar{C}_{Land}$, (b) vegetation carbon $\bar{C}_{Vegetation}$, (c) coarse woody debris carbon $\bar{C}_{WoodyDebris}$, (d) soil organic matter carbon $\bar{C}_{Soil}$ and (e) litter carbon $\bar{C}_{Litter}$ pools from 2015 to 2100 for the Bastin, Moustakis and Hurtt reforestation potentials compared to the baseline. A 15-year centered rolling mean was applied. Envelopes indicate one standard deviation across the five ensemble members. Note the different y-axes of the (d) and (e).

2 Drivers of temperature responses

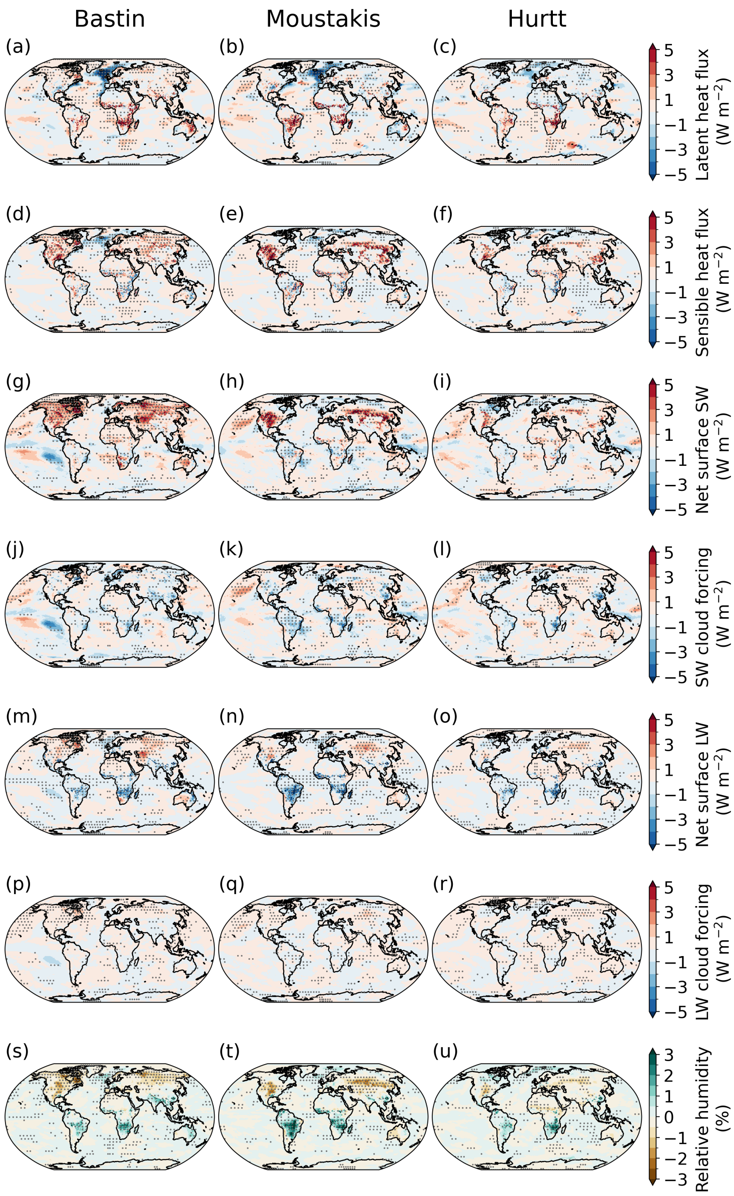

Fig. S2 Global maps of annual mean changes in (a-c) surface latent heat flux, (d-f) surface sensible heat flux, (g-i) surface net shortwave (SW) radiation, (j-l) surface shortwave cloud forcing, (m-o) surface net longwave (LW) radiation, (p-r) surface longwave cloud forcing and (s-u) relative humidity at the lowest model level from 2071 to 2100 for the ensemble mean of the Bastin, Moustakis and Hurtt potentials relative to the baseline. Stippling indicates regions where the response is statistically significant at the 90% level.

3 Seasonal temperature responses

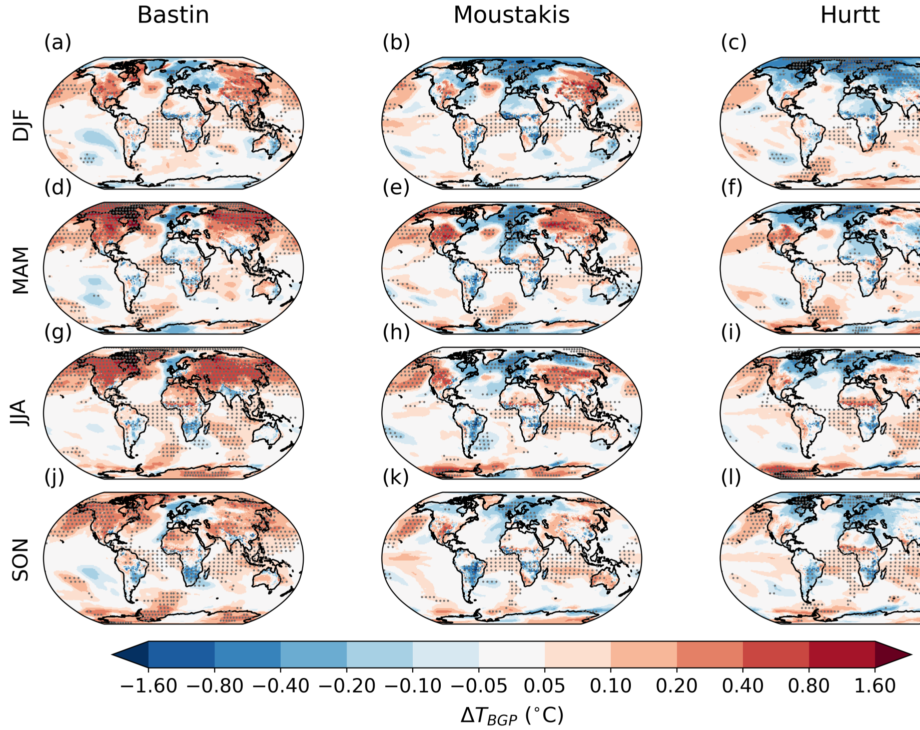

Fig. S3 Global maps of the BGP near-surface temperature changes in (a-c) December to February (DJF), (d-f) March to May (MAM), (g-i) June to August (JJA) and (j-l) September to November (SON) from 2071 to 2100 for the ensemble mean of the Bastin, Moustakis and Hurtt potentials relative to the baseline. Stippling indicates regions where the response is statistically significant at the 90% level.

4 Forest sensitivity

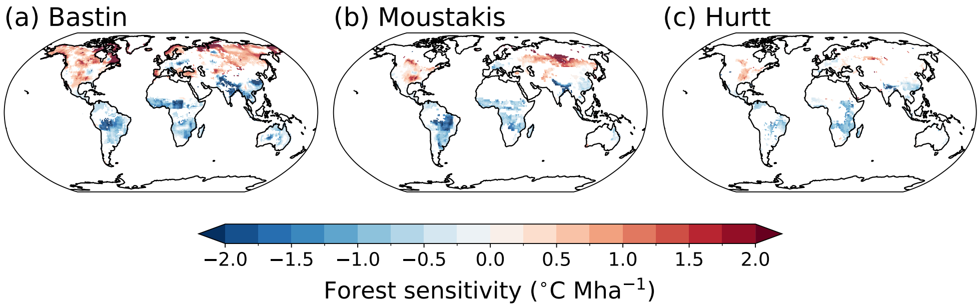

Fig. S4 Global maps of forest sensitivity (defined as ensemble mean local temperature response divided by forest cover area per gridcell) from 2071 to 2100 for the (a) Bastin, (b) Moustakis and (c) Hurtt reforestation potential relative to the baseline. Only regions where the local temperature changes by at least 0.025 °C are shown.

5 global-mean net temperature changes depending on different TCREs

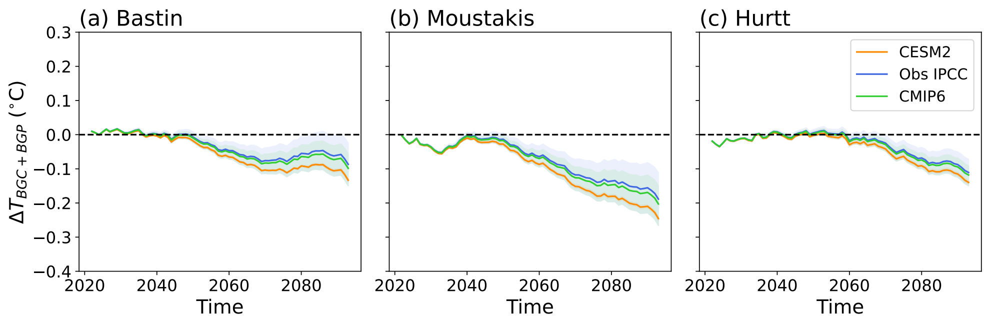

Fig. S5 Time series of global-mean near-surface temperature changes from 2015 to 2100 due to simulated biogeophysical (BGP) effects and calculated biogeochemical (BGC) effect for the (a) Bastin, (b) Moustakis and (c) Hurtt reforestation potential compared to the baseline. The BGC effect was calculated using the TCRE value from CESM2 (orange line; TCRE = 2.13 EgC^{-1}), from the best estimate based on observations as reported in the IPCC [1] (blue line; TCRE = 1.65 EgC^{-1}) and the mean value across CMIP6 models as reported in Arora et al. [2] (green line; TCRE = 1.77 °C EgC^{-1}). An 11-year centered rolling mean was applied. Envelopes indicate one standard deviation across the BGC temperature response for the calculation using the CESM2 TCRE, and the spread in the BGC temperature response based on the given spread in the observed TCRE values from IPCC (TCRE between 1-2.3 °C EgC^{-1} with a best estimate of 1.65 °C EgC^{-1}) and across CMIP6 models (TCRE between 1.32-2.3 °C EgC^{-1}). The spread based on the BGP temperature is not shown since it is the same for all three lines graphs. A 15-year centered rolling mean was applied to (a-c).

6 Global land cover transitions

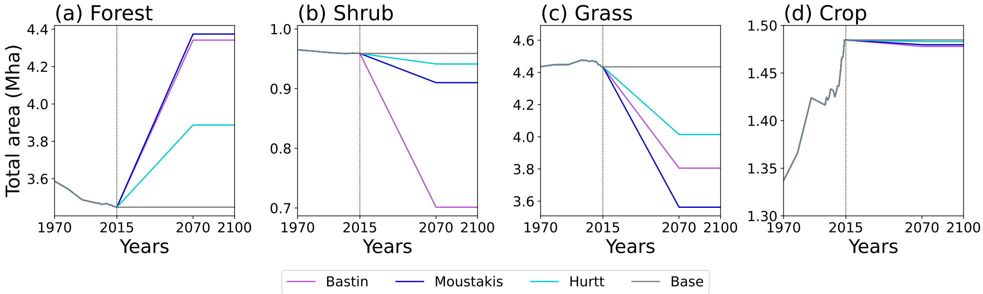

Fig. S6 Time series of global area covered by (a) forest, (b) shrub, (d) grass and (d) crop land for the baseline and the Bastin, Moustakis and Hurtt reforestation potential. In 2015, our simulations branch off from the historical simulations (dashed line).

7 Comparison of implemented reforestation potentials

Table S1 List of restoration potential datasets chosen in this study. Note that the total reforestation area values have been converted to Mha. The shorthand IAM stands for Integrated Assessment models.

Datasets	Bastin et al. [3]	Moustakis et al. [4]	Hurtt et al. [5]
Methods	Satellite and ground-based measurements combined with Machine Learning	Combination of >1200 IAM scenarios with reforestation potential maps from Griscom et al. [6] and Laestadius et al. [7]	IAM and land model to create forest map for LUH2
Assumptions and Safeguards	Excluded urban areas, current forest and cropland	Only afforested grazing land (i.e., pasture and rangeland) excluding natural grassland, shrubland and cropland. Constrained with map of low human influence.	Economic scenario
Total reforestation area	900 Mha	935 Mha	350 Mha for SSP1-2.6 at CESM2 resolution (and 440 Mha for SSP1-2.6 Max)
Total carbon uptake	205 GtC (750 $GtCO_2$)	380 $GtCO_2$	not given
Background climate	current climate (1970-2000)	SSP5-3.4os climate	SSP1-2.6 climate
Implementation in this study	Using restoration potential map (not global potential tree cover map)	Using change in forest fraction in 2100 compared to 2015 from MPI model	Using maximum forest cover increase from 2015 to 2100 (not difference in forest cover from 2100 to 2015)
Reforestation area implemented in CESM2	894 Mha	926 Mha	440 Mha

References

[1] Arias, P. A. *et al.* in *Technical summary* 33–144 (Cambridge University Press, 2021).

[2] Arora, V. K. *et al.* Carbon-concentration and carbon-climate feedbacks in CMIP6 models and their comparison to CMIP5 models. *Biogeosciences* **17**, 4173–4222 (2020).

[3] Bastin, J. F. *et al.* The global tree restoration potential. *Science* **365**, 76–79 (2019).

[4] Moustakis, Y., Nützel, T., Wey, H. W., Bao, W. & Pongratz, J. Temperature overshoot responses to ambitious forestation in an Earth System Model. *Nat. Commun.* **15** (2024).

[5] Hurtt, G. C. *et al.* Harmonization of global land use change and management for the period 850-2100 (LUH2) for CMIP6. *Geosci. Model Dev.* **13**, 5425–5464 (2020).

[6] Griscom, B. W. *et al.* Natural climate solutions. *P. Natl. Acad. Sci. USA* **114**, 11645–11650 (2017).

[7] Laestadius, L., Maginnis, S., Minnemeyer, S., Saint-Laurent, C. & Sizer, N. Mapping opportunities for forest landscape restoration. *Unasylva* **62**, 47–48 (2011).